Advanced Industrial and Engineering Polymer Research 9 (2026) 49–62

Contents lists available at ScienceDirect

Advanced Industrial and Engineering Polymer Research

journal homepage: http://www.keaipublishing.com/aiepr

Research paper

Dual interface strategies using carbon dots for fabricating thermally conductive polymers by pyrrhotite and waste plastics

Zhiyi Wang [a], Jianchao Wang [b,*], Hui Wang [a,**], Hongru Jiang [c], Chongqing Wang [d], Yingshuang Zhang [e], Hongshuai Hou [a], Lingyue Zhang [f]

[a] College of Chemistry and Chemical Engineering, Central South University, Changsha, 410083, Hunan, China
[b] State Key Laboratory of Nutrient Use and Management, College of Resources and Environmental Sciences, National Academy of Agriculture Green Development, Key Laboratory of Plant–Soil Interactions (Ministry of Education), China Agricultural University, Beijing, 100193, China
[c] Key Laboratory of Ministry of Education for Advanced Materials in Tropical Island Resources, School of Chemistry and Chemical Engineering, Hainan University, Haikou, 570228, Hainan, China
[d] School of Chemical Engineering, Zhengzhou University, Zhengzhou, 450001, China
[e] State Key Laboratory of Chemistry and Utilization of Carbon Based Energy Resources, Xinjiang Key Laboratory of Coal Clean Conversion & Chemical Engineering Process, School of Chemical Engineering and Technology, Xinjiang University, Urumqi, 830017, China
[f] Department of Civil Engineering, The University of Hong Kong, Pokfulam, Hong Kong SAR, China

ARTICLE INFO

Article history:
Received 25 July 2025
Received in revised form
22 August 2025
Accepted 10 September 2025

Keywords:
Polymer composites
Carbon dots
Thermal conductivity
Plastic recycling

ABSTRACT

The thermally conductive polymers used in modern microelectronic devices have been a hot topic around the world. Herein, we proposed a novel dual interface strategy to fabricate thermally conductive polymer with waste plastics and pyrrhotite (Pyr), and decipher the interface coupling mechanisms facilitated by carbon dots (CDs). First, through hot-pressing, the polymer composites (ABS/S@CD-Pyr) were fabricated using waste poly(acrylonitrile-co-butadiene-co-styrene) (ABS) and Pyr. The thermal conductivity (TC) of polymer composites was affected by various parameters, and the highest TC reached 1.68 W/m·K. Second, the interfacial coupling of ABS/S@CD-Pyr was elucidated via the systematical characterization and molecular dynamics (MD) simulation, and the chemical coupling (C–S and C═S bonds) and nanoscale effects of CDs were mainly responsible for the reduced interfacial thermal resistance and the enhanced thermal conductivity. Third, the other critical properties of polymer composites were estimated, and ABS/S@CD-Pyr possessed good electrical resistivity, electromagnetic interference shielding performance, thermal stability, mechanical strength, thermal cycling, and water resistance. Finally, the applicability of proposed strategy was tested with various types of waste plastics, and in most cases, the TC of polymer composites was above 1.60 W/m·K. These findings would provide valuable insights into the high-value resource utilization of waste plastics and Pyr tailings.

1. Introduction

As the keystone of electronic components in all electronic products, integrated circuits tend to be smaller, faster, lighter, and cheaper [1,2]. This urgently requires the materials used for electronic packaging with excellent thermal conductivity (TC), electromagnetic interference (EMI) shielding and electrical insulation [3]. Plastics and ceramic have been widely utilized in electronic packaging, and more than 90 % of electronic components are encapsulated by plastics. Nevertheless, most plastics have a low TC (0.1–0.5 W/m·K), and this defect is regarded as the critical bottleneck to the large-scale application of plastic packaging in the age of 5G [4,5]. Recently, thermally conductive polymers have attracted ever-increasing attention due to light weight, low cost, recyclability, and chemical stability, particularly for filling-type thermally conductive polymers [5,6]. This tactic is to incorporate fillers with high TC into polymer matrix, and thus the TC of polymer composites is affected by fillers. However, the widely used

* Corresponding author.
** Corresponding author.
E-mail addresses: jcwang91@163.com (J. Wang), huiwang1968@163.com (H. Wang).
Peer review under the responsibility of Kingfa Scientific and Technological Co., Ltd.

https://doi.org/10.1016/j.aiepr.2025.09.006

ceramic and carbon materials cannot take into account TC, electromagnetic shielding and insulation performance [7–11].

To address the exclusivity between TC and other key properties, the synergistic effects of multi-fillers have been explored. For example, Görkem and Meral [12] reported that aluminum nitride and boron nitride can improve the TC of polymers with good electrical insulation. In another study, Lee and Kim [13] reported similar findings using silver nanowire and aluminum nitride. However, this strategy suffers from great challenges due to the distinct properties of different fillers, leading to lower experimental TC than that of theoretical calculations of polymer composites. On the one hand, the large contact interfaces can increase the interfacial thermal resistance (ITR) between polymer matrix and fillers and the contact thermal resistance (CTR) between the fillers [14–16]. On the other hand, the homogeneous dispersion of fillers as a critical factor of thermal conduction is affected by the geometric factors of fillers, such as shape and size (but not limited) [14,17]. Based on the above intrinsic mechanisms, a few of proposals have been proposed; e. g., the covalent functionalization of fillers has been used to enhance TC via reducing ITR and CTR [18]. Nonetheless, proposing new strategies to improve the interfacial adhesion, as well as improve the dispersion of fillers in polymer composites still remains challenging [14].

Recently, inspired by the satisfactory compatibility of styrene-butadiene-styrene (SBS) with polystyrene matrix, we have proposed a bidirectional bridging strategy using the sulfurated SBS (S-SBS) to fabricate thermally conductive polymers [19]. The polymer composites exhibited a drastically enhanced TC, owing to the reduced ITR between the polyethylene matrix and S-SBS, along with the covalent coupling between S-SBS and pyrrhotite (as fillers). Nonetheless, due to the intrinsic thermal resistance, the relatively low TC of SBS bridging could restrict the thermally conductive performance of polymer composites. In this case, selecting thermally conductive materials for improving bridging would be a fascinating strategy to further enhance the TC of polymer composites. Carbon dots (CDs) have attracted increasing attention from various fields, although their practical application was restricted by high cost [20,21]. Interestingly, CDs exhibit a great compatibility with polymers and can increase the thermally conductive performance of resins due to nanoscale effects (i. e. effective penetration and dispersion) [22–24]. The rich functional groups of Ds make it a high-potential interface-coupling enhancer for the TC enhancement of filled polymer materials [25,26].

In recent studies, almost all thermally conductive polymers reported utilize the virgin polymers [27,28]. Plastics are one of the most widely used materials in various industries due to low cost, stability, diverse functionality, and moldability [29,30]. Poly(acrylonitrile-co-butadiene-co-styrene) (ABS) is a major component in electrical and electronic equipment; in particular, the content of ABS in cathode ray tube monitors reach up to 89 % [31–33]. An effective utilization of this part of waste polymers will bring environmental benefits [34,35]. Given the great demand for thermally conductive polymers, using waste plastics as raw materials would be of important significance with environmental and resource benefits. Pyrrhotite (Pyr) is an associated mineral of sulfide mineral, and it is always directly discarded in tailings ponds due to less iron and sulfur, leading to land occupation, severe soil acidification and erosion [36]. Given the polysulfide structures, semiconduction, and magnetism, we speculate that Pyr would be an ideal filler to prepare thermally conductive polymers with insulation and electromagnetic shielding [37–39]. In contrast to the costly nanomaterials used as fillers in most of literature [16,40], the utilization of cheap Pyr can address both disposal and pollution problems.

Therefore, this study aims to elucidate the interface-coupling enhancement mechanisms of CDs and evaluate the multiple capacities of thermally conductive polymers fabricated with waste plastics and Pyr tailings. For these purposes, the main objectives were **(a)** to investigate the effect of parameters on the TC of polymer composites, i. e. filler and CDs fractions, K_2S_n concentration, and factors in hot-pressing; **(b)** to ascertain the interface-coupling enhancement of CDs based on experiment and theoretical calculation; **(c)** to systematically evaluate the multiple capacities of polymer composites, along with the applicability using different waste plastics. To the best of our knowledge, this is the first report to elucidate the interface-coupling enhancement of CDs within thermally conductive polymers. These findings could provide mechanistic and technical insights into the design and application of thermal conductive polymers using waste plastics and tailings. Given the cheapness of raw plastic materials and that the production of CDs in kilogram scale has been established [41], the thermally conductive polymers have powerful application prospect.

2. Materials and methods

2.1. Materials

Waste ABS, polystyrene (PS), and polycarbonate (PC) were purchased from the plastic recycling market (Changsha, Hunan province of China). The pristine ABS resin (<40 μm) was purchased as comparison from Tingkai Co., LTD (Huizhou, Guangdong province of China). Pyr was collected after flotation of copper ores in mineral field (Anqing, Anhui province of China). The Pyr used in this study was obtained from the collected monoclinic Pyr through high-temperature phase transformation. The specific preparation details are as follows: The hexagonal Pry powder was prepared with the high-temperature phase transformation and quench by a typical water-cooled method. 50 g of monoclinic Pyr powder was packed in a quartz boat and heated in an atmospheric tube furnace with nitrogen gas for 30 min. The temperature rate was a 5°/min. After reaching 450 °C, the heat treatment was maintained for 12 h. After heat treatment, the obtained high-temperature powder was immediately quenched and cooled in ice-cold distilled water. The collected powder was filtered and finally dried under vacuum at 60 °C for 8 h and sealed for storage, and the obtained powder was recorded as hexagonal Pry. The more preparation details and the properties of Pyr are summarized in **Section S1** and Fig. S1 in Supporting **information**, respectively. Similar Pyr was also reported in our previous study **[**19**]**. The chemicals including ethyl alcohol, acetone, potassium polysulfide (K_2S_n), SBS elastomer, sodium hydroxide, sulfuric acid, nitric acid, hydrochloric acid, and oil-filled sulfur were analytic reagents and purchased from Aladdin Pharmaceutical Co., LTD (Shanghai, China). Multiwalled carbon nanotube (CNT) with diameter of 10–20 nm and length of 30–40 μm were provided by Aladdin Pharmaceutical Co., LTD (Shanghai, China). CDs were prepared via an aldol reaction reported in our previous study (**Section S2**) [41]. Then the active CDs was prepared in the following method: CDs (10 g) was carbonized by atmosphere tube furnace under N_2, and the heating rate was 10 °C/min. The carbonized CDs were obtained after being held at 900 °C for 20 h. The carbonized CDs were dispersed in a mixture of H_2SO_4 (98 %) and HNO_3 (68 %) with a volume ratio of 1:3 and then activated in a water bath at 85 °C for 60 min. Then, the activated CDs were washed with pure water and ethanol, filtered through a 0.22 μm polytetrafluoroethylene (PTFE) membrane, and dried at room temperature for 24 h. The deionized water prepared via reverse

osmosis based on an ultra-pure water machine was used throughout the experiments. Prior to fabricating thermally conductive polymers, the samples of waste ABS, PC, and PS, and monoclinic Pyr were pre-processed with the following procedures: waste plastics or monoclinic Pyr samples were cleaned with deionized water and dried at 40 °C for 24 h, crushed into fragments, and sieved through the 400 mesh. The crusher used can be seen in Fig. S2. Using monoclinic Pyr, hexagonal Pyr was prepared and used in this study to fabricate thermally conductive polymers [42].

2.2. Fabrication of ABS-S@CD-Pyr

The sulfuration of SBS and CDs (S-CDs) were performed prior to the fabrication of Pyr-filled thermally conductive polymer (ABS-S@CD-Pyr). The sulfurized SBS was prepared by mixing SBS and oil-filled sulfur and held at 70 °C for 15 min. The S-CDs samples were prepared via a typical hydrothermal method. In details, 1 g potassium polysulfide, 1 g activated CDs (see details in **Section S2**), and 50 mL deionized water were mixed and added into a PTFE-lined stainless-steel autoclave, heated and kept at 160 °C under a thermostatic oil bath for 24 h, and finally the S-CDs samples were obtained by washing centrifugation and drying under room temperature.

The ABS-S@CD-Pyr samples were fabricated by following procedures (Fig. 1). Firstly, S-CDs was added into 30 mL ethanol and treated using ultrasound for 5 min, Pyr was added and treated using ultrasound for 5 min, and then the mixed mixture of ABS and sulfurized SBS with a mass ratio of 3:1 was added and treated using ultrasound for 5 min. Secondly, the mixtures were filtered via the 0.22 μm polytetrafluoroethylene membrane, dried under vacuum at 40 °C for 24 h, and grounded for 15 min using an agate mortar. Finally, the samples were subject to hot-pressing in a self-designed equipment and various ABS/S@CD-Pyr were fabricated under different material ratio and hot-pressing conditions: the fraction of Pyr (50–95 wt%), the fraction of S-CDs (0.5–2.5 wt%), hot-pressing temperature (170–270 °C), hot-pressing pressure (6–21 MPa), and hot-pressing time (10–40 min). The adoption of this hot-pressing temperature range during the experiment is mainly due to the fact that ABS is the main matrix of the composite material. The heat distortion temperature of ABS is 110–120 °C, and its pyrolysis temperature is 250–280 °C (depending on different plasticizing additives). Too low or too low hot-pressing temperature will cause the composite material to fail to form. Too low a hot-pressing temperature is also not conducive to the occurrence of interfacial reactions, while too high a hot-pressing temperature will cause varying degrees of thermal decomposition of ABS, thereby destroying the thermal conduction network. For comparison, CNT was utilized to fabricate ABS/S@CNT-Pyr under similar procedures. Note that for easily measuring the capacities of thermally conductive polymers, ABS-S@CD-Pyr was processed to round sheet with a diameter of 20 mm and a thickness of 5 mm) or rectangular sheet (length is 20 mm, width is 10 mm, and height is 5 mm).

2.3. Characterization

The morphological features were recorded by scanning electron microscope (SEM, MIRA3 TESCAN, Czech Republic) after gold spraying. The microstructural features were measured by transmission electron microscopy (TEM, JEM2010, Japan Electronics Co., LTD, Japan). The functional groups were ascertained by Fourier transform infrared spectroscopy (FT-IR, Nicolet 6700, Thermo Fisher Scientific, USA). The crystallization was determined by X-ray diffraction (XRD) using Cu Kα ($\lambda = 0.15418$ nm) radiation source (D8Advance, Bruker, Germany). The surface compositions were measured by X-ray photoelectron spectra (XPS, Thermo Scientific K-Alpha, England). The thermogravimetric and differential thermal analyses (TGA, DSC) were measured with TGA (TGA-2-SF/1100, Mettler Toledo) and DSC analyzers (DSC 3/DSC 3+), respectively. Within measurement, the temperature rate was 10 °C/min from 30 to 300 °C under N_2 atmosphere.

By using Transient Plane Source Method (TPS) according to the ISO 22007-2008 standard, the TC values of polymer composites were recorded using a Hot Disk thermal analyzer (Hot Disk 2500-OT, Sweden). At least triplicate measurements were recorded in all experiments. The infrared thermal imaging was recorded using an infrared thermal imager (FLIR-E4, Teledyne FLIR). Raman spectrum imaging was recorded by a Raman spectrometer (MacroRAM). The electrical resistivity of polymer composites with a 20 mm

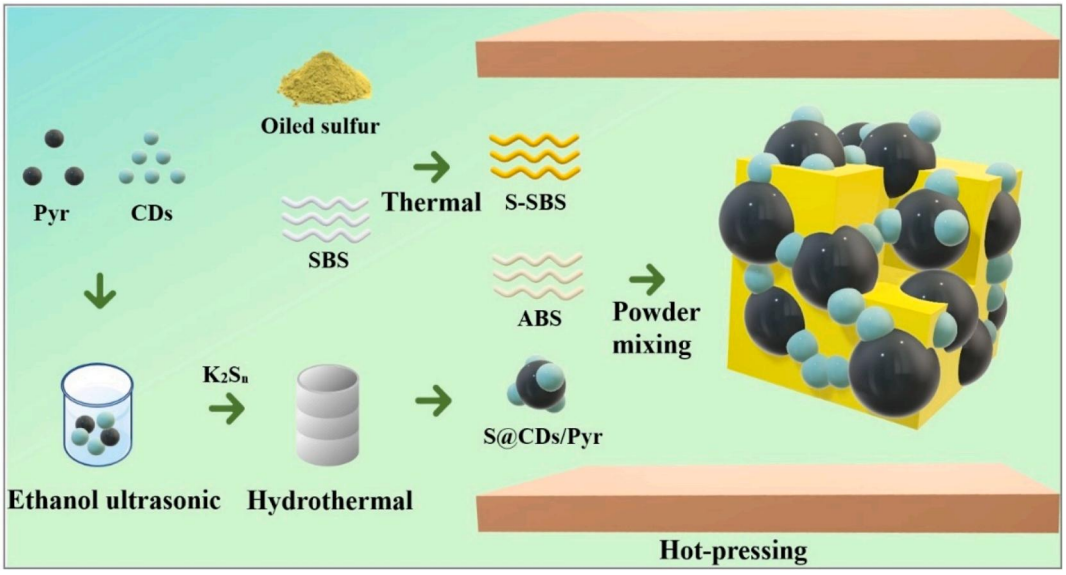

Fig. 1. The schematic diagram for fabrication of ABS-S@CD-Pyr samples.

diameter and a 5 mm thickness was measured with a Keithley 6480 Picoammeter (Keithley, USA) under a constant voltage of 1 V. The EMI shielding coefficient and tangent of the dielectric loss angle were measured by a vector network analyzer (AV3629, China Electronics Science and Technology Corporation) in the band of 8–12 GHz. The polymer composites were precisely cut to 22.86 mm × 10.16 mm × 2 mm and tested by wave-guide method. The single column and single arm electronic tensile testing machine (LDS-5) was used to evaluate the tensile strength. The selected tensile rate was 5 mm/min.

2.4. Simulation methods

Given that the molecular dynamics (MD) simulation can provide a closer observation of the details of the interfacial transport phenomena than physical experiments, it was used to study the thermal transport of polymer composites. The MD simulation of polymer composites was performed using nonequilibrium molecular dynamics (NEMD) with the large-scale molecular massively parallel simulator (LAMMPS) package [43,44]. The timestep was chosen to be 0.25 fs, and a 10 Å cutoff was used for 6–9 Lennard-Jones (L-J) potential, allowing for chain-chain interactions between the third and fourth nearest-neighboring chains. The temperature gradient was created and maintained by Langevin thermostats controlling the temperatures of the two ends of the simulation domain. The temperatures of the heat sink and heat source regions were set to 15 K lower and higher than the average system temperature, respectively. The condensed-phase optimized molecular potentials for atomistic simulation studies (COMPASS) and the universal force field (UFF) were utilized to model polymers and CDs, and Pyr molecules, respectively. To make fair comparison among different materials, the materials were constructed by controlling the number of the segments in polymer chains so that the simulation domain lengths were around 50 nm at 300 K. From the minimized structures, the systems were simulated Isothermal-isobaric (NPT) ensembles for 1 ns with 1 atom.

3. Results and discussion

3.1. The effect of components' fractions on thermally conductive performance

The fraction of fillers in polymer composites can strongly determine the thermally conductive performance [45,46]. In this regard, the effects of various components' fractions and hot-pressing parameters on the TC values of polymer composites were investigated systematically (Fig. 2). It is necessary to note that for comparison, the effect of CNT, as another interface-coupling enhancer, on the TC of polymer composites was included, since CNT with exceptional thermal (≈3000 W/m·K) and mechanical properties has been widely utilized as fillers of thermally conductive polymers [9,47]. As displayed in Fig. 2a, the TC values of all polymer composites increased continuously with the fractions of Pyr, and there was a summit for various polymer composites. When the fraction of Pyr was 88 wt%, ABS/S@CD-Pyr had the largest TC (1.68 W/m·K), much greater than that of other polymer composites. In particular, ABS/CD-Pyr (even if CD was not sulfurized) possessed greater TC than that of both ABS/S@CNT-Pyr and ABS/CNT-Pyr. These results clearly demonstrated that in contrast to CNT, CDs was a more effective interface-coupling enhancer for improving the TC of polymer composites. Son et al. [24] reported similar findings for the impact of CDs on the thermal conductive performance of carbon nanosheets. This was mainly attributed to the greater compatibility of CDs with polymers and the nano-size effects, leading to the uniform dispersion of CDs in polymer matrix [48–50]. In another study, the disordered dispersion of CNT in polymer matrix has been reported by Yu et al. [51], as a critical issue of CNT-filled thermally conductive polymers. This physical effect of CDs was expected to strengthen the interfacial coupling of fillers with polymers.

In addition, we found that the presence of CDs obviously increased the filling fraction of Pyr, and the highest TC of ABS/S@CD-Pyr and ABS/S@CNT-Pyr was reached with Pyr fraction of 88 wt% and 78 wt%, respectively. The content of fillers in polymer composites is generally limited to be less than 20 % due to possible aggregation [52]. However, in our case, the fraction of Pyr was substantially increased, possibly attributed to the well-dispersed fillers facilitated by CDs. For all the fractions of Pyr tested, the TC of ABS/S@CD-Pyr was much greater than that of ABS/CD-Pyr. Likewise, similar treads were found for counterparts containing CNT. This manifested that the sulfurization exhibited an obvious enhancement for the TC of polymer composites, and particularly such an effect was more markedly for CDs. To decipher this phenomenon, we further studied the effect of K_2S_n concentration during the sulfurization on the TC of polymer composites (Fig. 2b). It was observed that as K_2S_n concentration increased to 24 g/L, the TC of ABS/S@CD-Pyr increased steadily to 1.68 W/m·K, and afterwards the increased K_2S_n concentration displayed a strongly negative effect. Similarly, the increased K_2S_n (0–12 g/L) showed a slight enhancement on the TC of ABS/S@CNT-Pyr, and subsequently a reduction effect was found. The reasons were because the excess K_2S_n could induce the more precipitates, and thereby the newly formed interfaces would increase the ITR, in agreement with the previous reports [19].

On the other hand, due to the great compatibility and nano-size effect of CDs, the well-dispersed sulfurized CDs was inclined to bridge the interfacial void and to strength the interfacial coupling between Pyr and polymer matrix [25,50]. Meanwhile, the more sulfur-bearing moieties formed on the surface of CDs would endow it with strongly chemical interactions to reduce both the ITR between fillers and polymer matrix and the CTR between fillers [53,54]. As a result, the TC of polymer composites induced by the sulfurization of CDs was much greater than that of CNT. The effect of CDs or CNT fractions on the TC of polymer composites was further investigated (Fig. 2c). It can be seen that as CDs or CNT fractions increased, the TC of polymer composites firstly increased and then decreased; the TC of ABS/S@CD-Pyr and ABS/S@CNT-Pyr achieved maximum at the CDs and CNT of 1.5 wt% and 2.0 wt%, respectively. The greater TC of polymer composites at lower-fraction of CDs than that of CNT was possibly attributed to the small size of CDs. The lower TC of polymer composites at higher-concentration CDs or CNT was due to the disordered dispersion [46]. Generally, the findings provided preliminary evidence for the speculation made in **1. Introduction** that CDs would be an effective interface-coupling enhancer for enhancing the TC of Pyr-filled polymer composites due to physical and chemical effects. Nevertheless, the more convincing evidence of mechanistic details for the speculation is still needed.

3.2. The effect of hot-pressed conditions on thermally conductive performance

Wang et al. [55] reported the parameters of hot-pressing impacted the homogeneity of polymer composites. Therefore, the effect of parameters in hot-pressing treatment on the TC of polymer composites was investigated (Fig. 2e–g). It was clearly seen that in almost all cases, increasing the temperature, pressure, and time of hot-pressing treatment exhibited a positive impact on the TC of polymer composites. In general, under high temperature

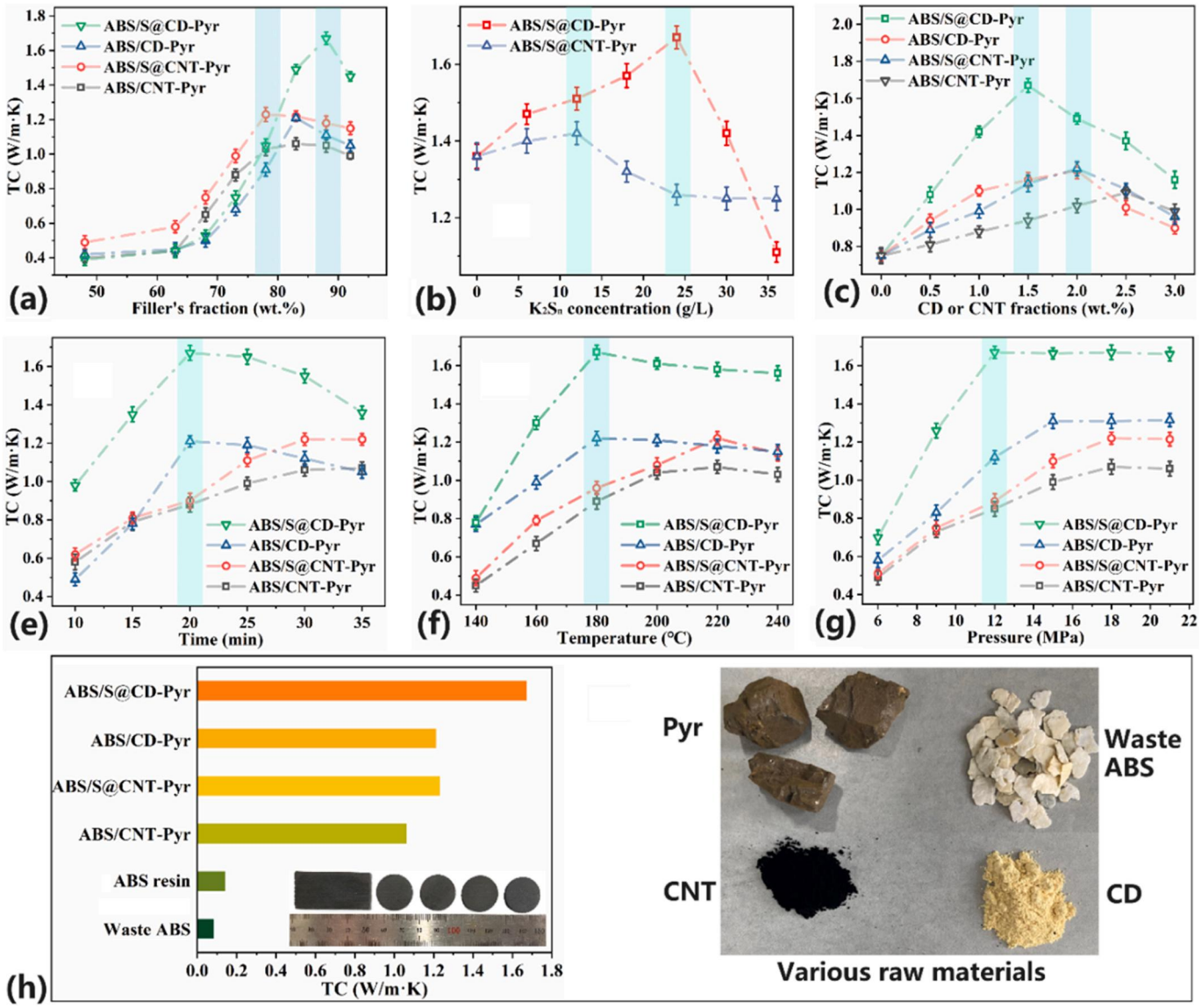

Fig. 2. The effect of fillers' fractions **(a)**, potassium polysulfide concentration **(b)** during sulfurization, CDs or CNT fractions **(c)**, along with time **(e)**, temperature **(f)**, and pressure **(g)** in hot-pressed treatment; the TC values **(h)** of various polymer composites and polymers, along with the images of raw materials.

and pressure, the fluidity of polymer matrix could be improved, and the physical spaces of interphase boundary of fillers with polymer matrix would be reduced, promoting the fabrication of homogeneous system and the formation of more strongly interfacial coupling. However, there were extremities for enhancing the TC values of polymer composites by increasing the parameters of hot-pressing treatment. These results are in agreement with the thermally conductive polymers containing the expanded graphite network reported by Wei et al. [56] and with graphene aerogel reported by Zhang et al. [57]. In details, the TC of ABS/S@CD-Pyr and ABS/CD-Pyr reached the highest values under 20 min, 180 °C, and 12 MPa, and 20 min, 180 °C, and 15 MPa, respectively. Within all range of conditions tested, the polymer composites with CDs had greater TC than that of the counterparts with CNT. More importantly, the conditions to achieve the highest TC values of the polymer composites with CDs were more moderate than that with CNT. These findings provided more convincing evidence for the more effective interface-coupling of CDs than that of CNT, as discussed in the above sections. The comparison of TC between the polymer composites along with the raw materials (including waste ABS and pristine ABS resin) was performed, as displayed in Fig. 2h. It can be found that the TC of polymers was substantially enhanced by the filling of Pyr along with the interfacial enhancement of CDs; the corresponding enhancement efficiency exceeded about 1988 %.

3.3. Characterization of polymer composites

3.3.1. SEM measurements

To illustrate the dispersion and interfacial features of fillers in polymer matrix, we recorded the SEM images of polymer composites, as well as the TEM of CNT and CDs (Fig. 3 and Figs. S3–4). It was clearly observed that CNT showed multi-walled features with a tube diameter of approximately 15 nm, in line with the widely used counterparts in CNT-filled thermal polymers [47,51]. The TEM images showed that CDs were well-dispersed with a diameter of about 5 nm. Overall, it was found that ABS/S@CD-Pyr exhibited a more homogenous structure than that of ABS/S@CNT-Pyr. As illustrated in Fig. 3a, ABS/S@CD-Pyr exhibited a relatively smooth surface with the well-distributed fillers (Pyr) in polymer matrix.

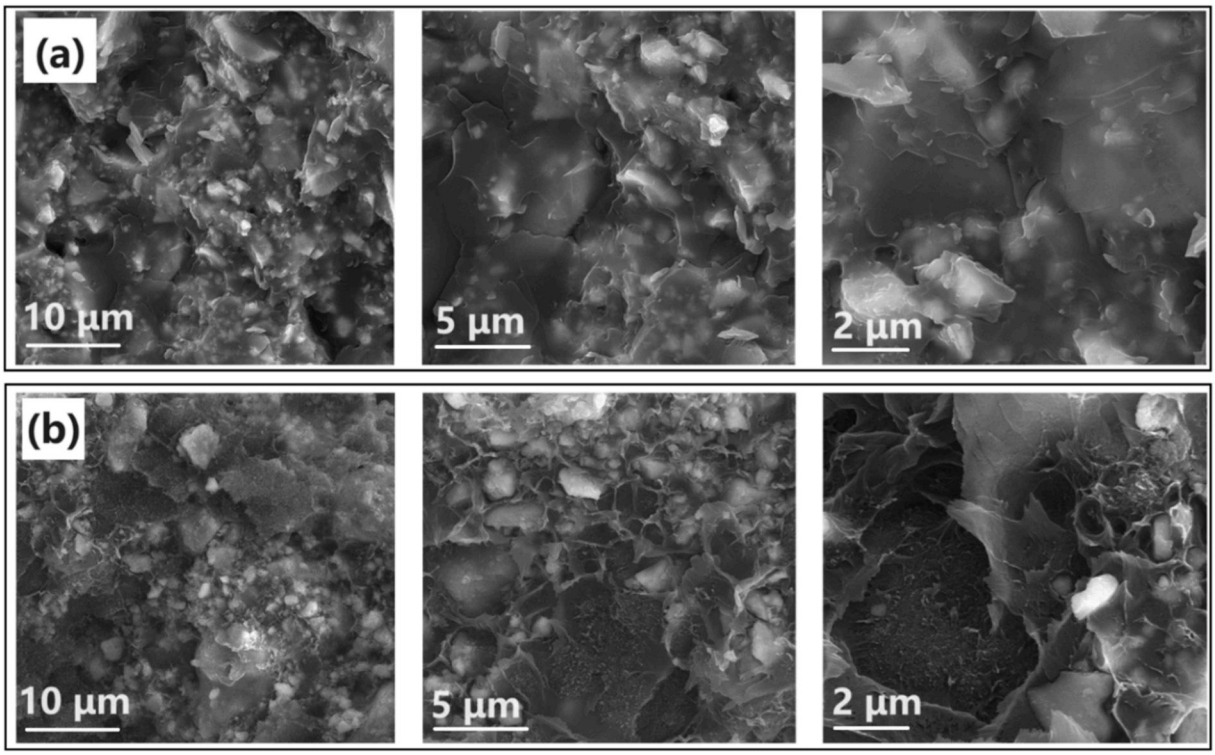

Fig. 3. The SEM images of ABS/S@CD-Pyr **(a)** and ABS/S@CNT-Pyr **(b)** with various magnitudes.

Importantly, it was apparent that the fillers were encapsulated by polymer matrix. These results provided solid evidence that the presence of CDs (although it cannot be observed) promoted the compatibility of Pyr and the polymers and the formation of extremely homogeneous polymer composites. In comparison, ABS/S@CNT-Pyr showed a rough morphology with some irregular particles and threadiness clusters; the former was the Pyr, and the latter was the clustered aggregates of CNT. Such dispersion and interfacial features clearly demonstrated that CNT failed to fabricate the homogeneous system of polymer composites. This was in good agreement with the previous reports for the unordered distribution of CNT in polymers due to agglomeration and low compatibility [58]. In this case, in contrast to CNT, the reduced interfacial distance and the enhanced interfacial coupling induced by CDs were envisioned to fabricate the effective thermal-conductive network.

3.3.2. XRD patterns

The crystallographic structures of polymer composites were characterized by using XRD patterns (Fig. 4a). It was obvious that the XRD of Pyr displayed a series of diffraction peaks centered at 29.9°, 30.2°, 33.4°, 30.2°, 35.6°, 43.2°, 57.3°, and 62.6°, which were characteristic diffraction peaks of hexagonal pyrrhotite (PDF#24–0220). After filling into the polymer matrix, the diffraction peaks of Pyr were still prominent in all composites due to the high fraction of Pyr in polymer composites. More interestingly, using CDs or CNT as the interface-coupling enhancers, it was found that the intensity of peaks at 30.2°, 35.6°and 62.6° increased apparently, demonstrating that the reactions occurred between these crystal planes and CDs or CNT [59]. The results of feature sharpening also indicate that this type of reaction leads to a higher degree of crystallinity at this interface. This phenomenon of increased crystallinity may be similar to the process of natural rubber vulcanization-induced crystallization. Importantly, these changes in the intensity of these diffraction peaks were more prominent for CDs than that for CNT, and this phenomenon was strongly promoted by the sulfurization for both CDs and CNT. These findings clearly demonstrated that in comparison with CNT, the interface-coupling enhancement between the fillers and polymer matrix induced by the sulfurized CDs were more effective, in good agreement with the TC values of polymer composites.

3.3.3. FT-IR and Raman spectra

The changes in the functional groups of polymer composites were determined using FT-IR spectra (Fig. 4b). In the FT-IR spectrum of waste ABS, the characteristic bands at 2989 cm^{-1} and 2848 cm^{-1}, 2911 cm^{-1}, 2120 cm^{-1}, 1626 cm^{-1} and 1447 cm^{-1}, and 1493 cm^{-1} were attributed to the ethylene, aromatic ring, acrylonitrile, stretching in the aromatic ring, and nitrile group, respectively [31,60]. After fabricating polymer composites, most of typical FT-IR bands of ABS declined, mainly due to the high fraction of fillers. It was very interesting that some new bands at 477 cm^{-1}, 570 cm^{-1}, and 806 cm^{-1} appeared in the FT-IR spectra of polymer composites, primarily corresponding to the C–S and C═S groups [61,62]. This was consistent with a recent study reported by Zhao et al. [63] that the sulfur-containing groups were incorporated in polymer composites via a similar hot-pressing treatment. Raman spectra were recorded to ascertain the interface coupling of polymer composites (Fig. 4c). In good agreement with the results of XRD and FT-IR, it was found in the Raman spectra of polymer composites that two newly formed peaks at 864 cm^{-1} and 1052 cm^{-1}, which were the stretching vibration of C–S and C═S groups [64,65]. It was reasonable to speculate that there was covalent bonding between S-CDs, Pyr, S-SBS, and waste ABS.

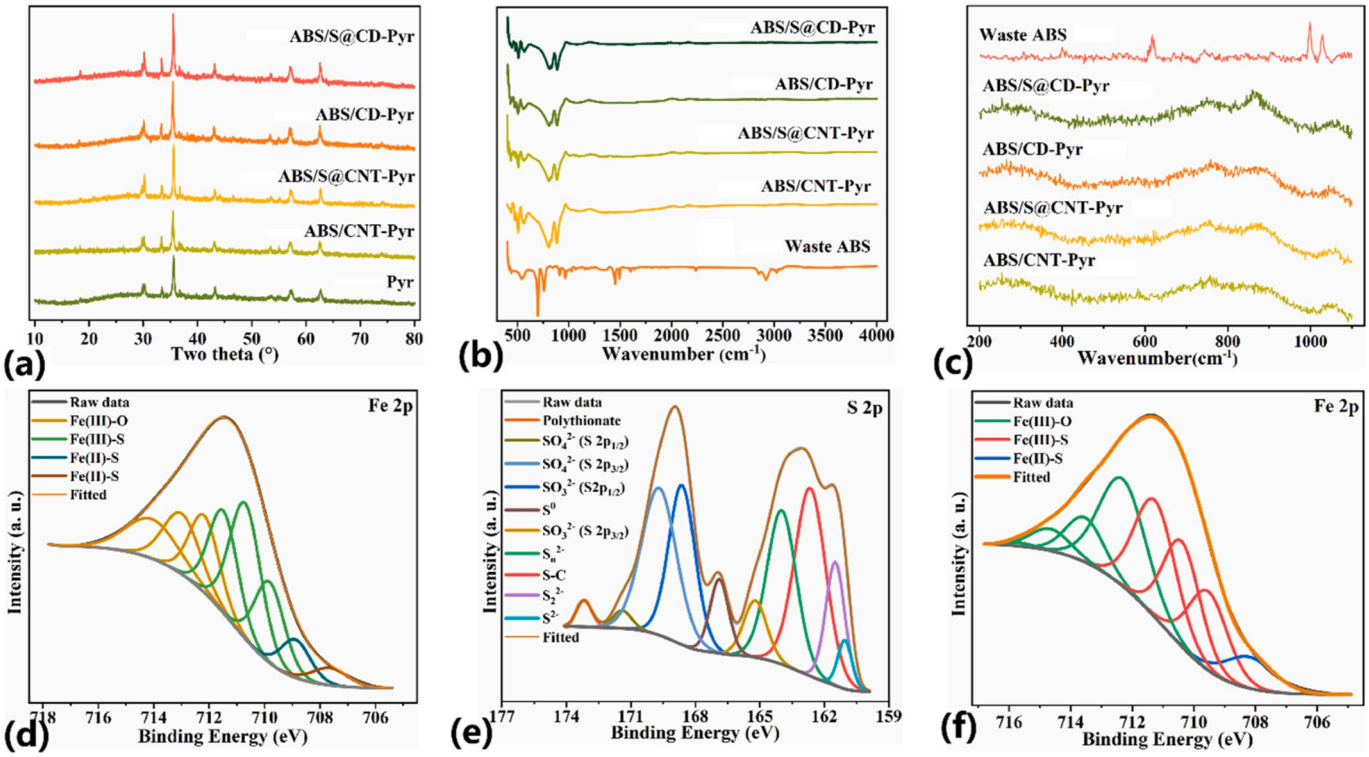

Fig. 4. The XRD patterns **(a)**, FT-IR spectra **(b)**, and Raman spectra **(c)** of polymer composites and raw materials; the XPS Fe 2p high-resolution region **(d)** and S 2p high-resolution region **(e)** of ABS/S@CD-Pyr; the XPS Fe 2p high-resolution region **(f)** of ABS/CD-Pyr.

3.3.4. *XPS analysis*

To verify the speculation, the XPS spectra along with the high-resolution Fe 2p and S 2p regions of ABS/S@CD-Pyr and ABS/CD-Pyr were determined to ascertain the chemical states of elements (Fig. 4d–f and Fig. S5). The relative proportion of fitted-peaks in the high-resolution Fe 2p and S 2p regions was summarized in Tables S1–2. Both for these two polymer composites, the high-resolution Fe 2p was dominated by Fe(III)–O, Fe(III)–S, and Fe(II)–S peaks at binding energy of 714.7-707.6 eV. The Fe(III)–O) peak was possibly due to the oxidation reactions during the preparation of Pyr [38]. In comparison, a new peak at 707.6 eV [Fe(II)–S] was found in the high-resolution Fe 2p region of ABS/S@CD-Pyr. This firmly manifested the reactions of S-CDs with the Fe of Pyr. In the high-resolution S 2p, polythionate, SO_4^{2-} (S $2p_{1/2}$), SO_4^{2-} (S $2p_{3/2}$), SO_3^{2-} (S $2p_{1/2}$), S^0, SO_3^{2-} (S $2p_{3/2}$), S_n^{2-}, S–C, S_2^{2-}, and S^{2-} at 173.3–159.0 eV were identified [37]. In particular, the relative proportion of S–C in high-resolution S 2p region of ABS/S@CD-Pyr was high to 22.32 %, much greater than that of ABS/CD-Pyr (Tables S1–2). One possible reason for this phenomenon was that S-CDs promoted the formation of more S–C moieties in interfaces than that of CDs. The presence of S–C moieties was in agreement with the findings of XRD, FT-IR, and Raman analyses, providing convincing evidence for the above speculation. Based on the analyses above, combined with the TC of polymer composites, it can be concluded that S-CDs was the effective interface-coupling enhancer to increase the TC of Pyr-filled polymer composites via both physical and chemical effects. For the former, as confirmed by SEM images, the introduction of S-CDs facilitated establishing the highly homogeneous system; for the latter, the formation of C–S and C═S groups in the interfaces of polymer composites was induced by adding S-CDs, as supported by XRD, FT-IR, Raman, and XPS results. These two main effects provided direct evidence for the speculation in **Introduction** and were envisioned to reduce ITR and CTR, enhancing the TC of polymer composites [28,58].

3.4. *MD simulation of interface transport of polymer composites*

The MD simulation was performed to provide mechanistic insights into the interaction of Pyr with ABS, S-CDs, and S-SBS. We found in the 3D differential charge density map (Fig. 5a–c and Fig. S6) that in all cases, the presence of efficient coupling was observed. The electron loss and gain regions gathered on the sulfuration moieties of S-SBS and S-CDs, while this was not observed between Pyr and ABS. This manifested the strong chemical coupling occurred on the sulfuration moieties of S-SBS and S-CDs. Similar findings focusing on chemical coupling (C–S and S–S) between the sulfurated carbonaceous materials have been reported by Ren et al. [53] and Deliballi et al. [54]. In particular, the higher charge density was found between Pyr and S-CDs, suggesting the strong chemical interactions. As shown in Fig. 5d–f, Pyr/S-SBS possessed high phonon density of states and mean free path, manifesting that the energy loss of phonon induced by collision and the ITR were reduced. Pyr/S-CDs exhibited greater phonon group velocity, suggesting the enhanced interfacial interactions. Using MD simulation, Luo and Lloyd [44] ascertained that the interface interactions greatly affected the efficiency of thermal transport, and the strong interactions resulted in larger interfacial thermal conductance. In this regard, the reduced ITR and the enhanced interactions are envisioned to enhance the interfacial thermal conductance, in good agreement with the experimental results. Likewise, these above findings were supported by the results of volumetric heat capacity along with temperature changes of thermal diffusion (Figs. S7–8). Clearly, constructing stronger C–C bonds directly between polymers and inorganic substances usually requires harsh reaction conditions, whereas building chemical interactions between C and S is

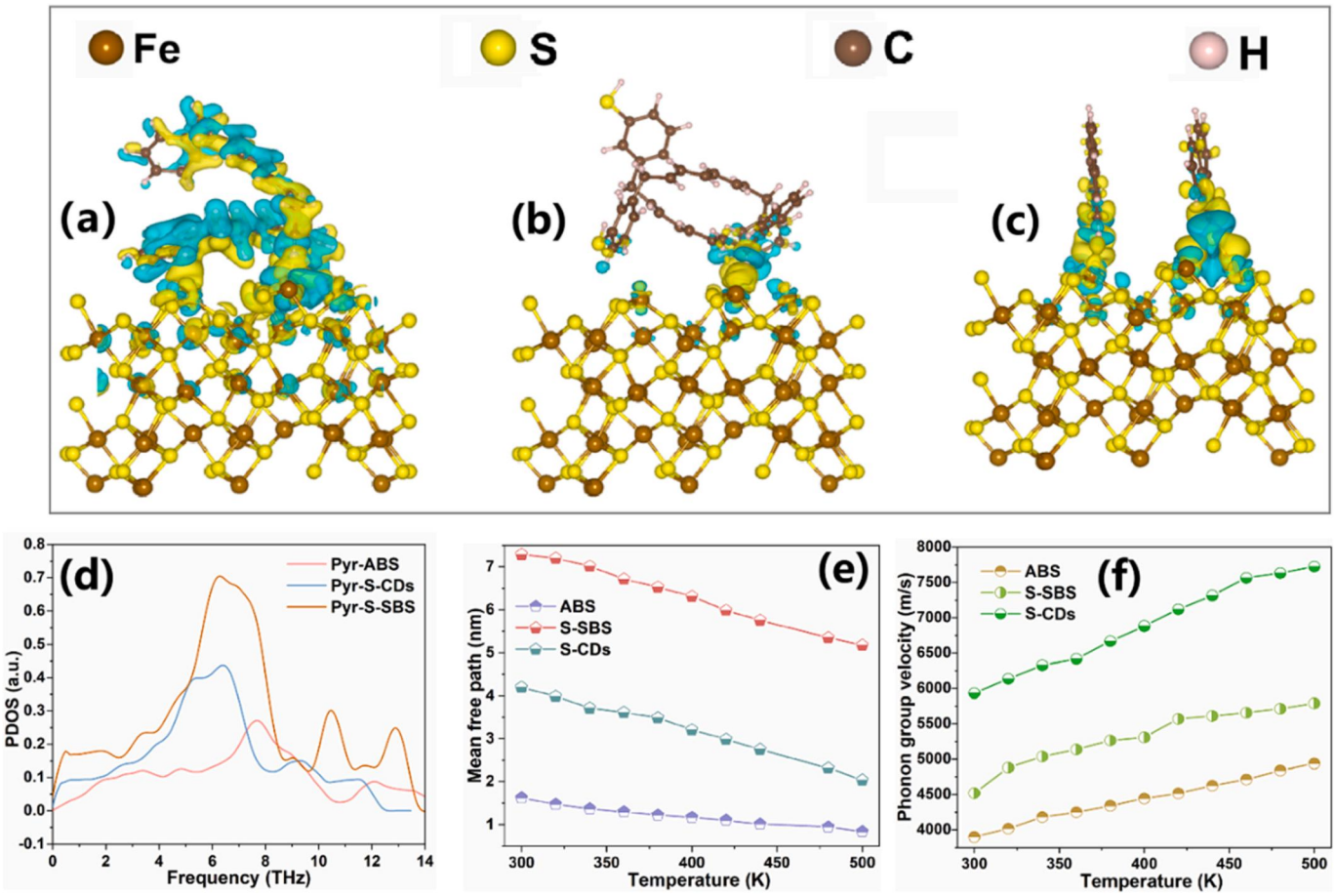

Fig. 5. The 3D differential charge density map of Pyr with ABS **(a)**, S-SBS **(b)**, and S-CDs **(c)**; herein, the cyan regions indicate a decrease in electron density (electron loss), while the yellow regions represent an increase in electron density (electron gain); the phonon density of states **(d)**, phonon mean free path **(e)**, and phonon group velocity **(f)** of Pyr with ASB, S-SBS, and S-CDs.

relatively straightforward. The bond energy of C–S is around 272 kJ/mol, whereas that of C═S is approximately 573 kJ/mol. The bond length of C–S is approximately 182 p.m., while that of C═S is 160 p.m. In terms of chemical bond energy, the covalent interactions resulting from the bond energies of C–S and C═S are far greater than the electromagnetic and van der Waals forces that occur when the two substances come into direct contact. This stronger interaction force effectively reduces the scattering of dissonant phonons, thereby lowering the interfacial thermal resistance [66]. This is precisely the key factor affecting the heat transfer performance of filled thermal conductive polymers.

3.5. Mechanisms of CDs-induced interface-coupling enhancement

Based on the above experimental and theoretical calculation results, the interface-coupling enhancement mechanisms of S-CDs were proposed. The nanoscale effect and great compatibility endow CDs with efficient penetration, exhibiting a good fit with both Pyr and the polymer matrix via chemical bonding and size fitting, as illustrated in Fig. 6. It has been established that using fillers with various sizes and covalent functionalization were two main strategies for enhancing TC of polymer composites [1,5]. However, the interfacial voids formed between polymer matrix and fillers severely restrict the availability of the covalent functionalization strategy. In our study, the uniform and nanoscale CDs possessed high specific surface area and increased the contact area with the other components. In this case, CDs would strongly reduce the distance between molecular chains of polymer and fillers, and thereby the success probability and effectiveness of fabricating chemical interactions would be greatly improved. Based on this, S-CDs would possess the combined advantage of the two main aforementioned strategies for enhancing TC of polymer composites. In a typical scenario, the following interface interactions were present: **(a)** Pyr directly interacted with the polymer matrix (ABS/S-SBS homopolymer); **(b)** the nanoscale S-CDs effectively covered the surface of Pyr; **(c)** the composites with S-CDs and Pyr interacted with the polymer matrix. In the first interaction, due to the large size of Pyr, the number of polysulfide bonds formed was generally limited. By contrast, in the second interaction, numerous polysulfide and C–S/C═S bonds were formed (as demonstrated by the above results) due to the nanoscale effect of S-CDs and the polysulfide moieties of Pyr. In the third interaction, the C–S/C═S bonds between S-CDs and the polymer matrix can be formed, which was evidenced by the results of MD simulation. Based on these interactions, the uniformly-distributed S-CDs in the polymer matrix fabricated an effective bridge for enhancing the interfacial coupling of Pyr with polymers, and in this case ABS/S@CD-Pyr possessed great prominent thermally conductive performance.

3.6. The performance evaluation for practical application

For practical application of thermally conductive polymers, the performance of thermal conduction, insulation performance, thermal stability, mechanical properties, and hydrophobicity is of

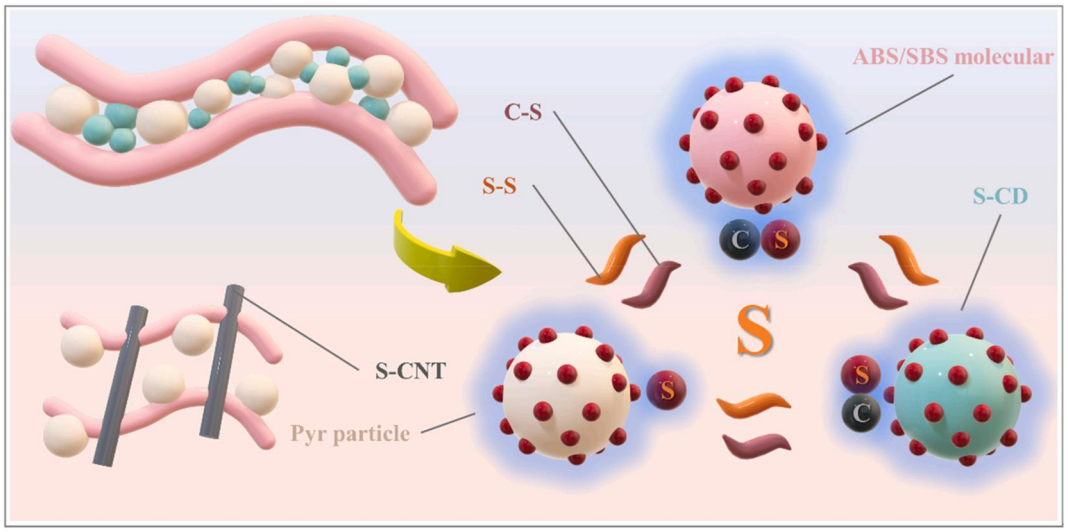

Fig. 6. The mechanisms of interface-coupling enhancement induced by CDs towards the TC enhancement of polymer composites.

significant importance. For instance, the electrical and electronic equipment including switches, waterproof partitions, and frame materials has specific requirements for insulation, hydrophobicity, and mechanical strength, respectively. In this regard, to evaluate the practical performance of polymer composites in our study, the multiple practical performances need to be evaluated.

3.6.1. *The simulation heating diffusion*

The simulation experiment was performed focusing on the chip heat diffusion for practical application of thermally conductive polymer composites. As showed in Fig. 7a, a polyimide heating film with power of 5 W and thickness of 1 mm was placed within two identical composite polymers (prepared in our study) to simulate the heat diffusion scenario of a chip and its packing materials in a typical electrical and electronic equipment. The experiment setup was placed on the insulating foam board at a temperature of 25 °C. The procedures of simulation experiment were: the polyimide film was heated for 15 min and then was subject to natural cooling. During the heating and cooling process, the surface temperature of the simulated device was recorded by an infrared camera.

The thermal imaging of simulated device is shown in Fig. 7b. For raw material (waste ABS), it can be seen that the thermal response started from approximately 30 s, and reached maximum temperature (78 °C) after 15 min heating; after natural cooling for 5 min, its temperature was high at 42 °C. By contrast, the heating response, maximum temperature, and natural cooling rate of polymer composites exhibited clear improvement. Particularly, a greater thermal response of ABS/S@CD-Pyr was found, and after heating for about 15 s, its temperature reached 28 °C, indicating that its thermal response time was less than 15 s. Importantly, the maximum temperature of ABS/S@CD-Pyr was 35 °C after heating for 1min, much lower than the maximum operating temperature of most electrical and electronic equipment. After natural cooling for 1 min, the temperature of ABS/S@CD-Pyr decreased to 25 °C. These results manifested that ABS/S@CD-Pyr possessed a greater thermally conductive performance than that of other polymer composites. It should be noted that in our experiment, one side of the polymer composites was exposed to air and possessed heat exchange with the environment. However, for actual electrical and electronic equipment, both two sides of the chips are often in contact with solid components, which are envisioned to improve the heat exchange. In this case, it can be concluded that the polymer composites (particularly for ABS/S@CD-Pyr) showed great practical application potential.

3.6.2. *The electrical resistivity*

The good electrical insulation of the thermally conductive polymers is another key property and needs to be considered for

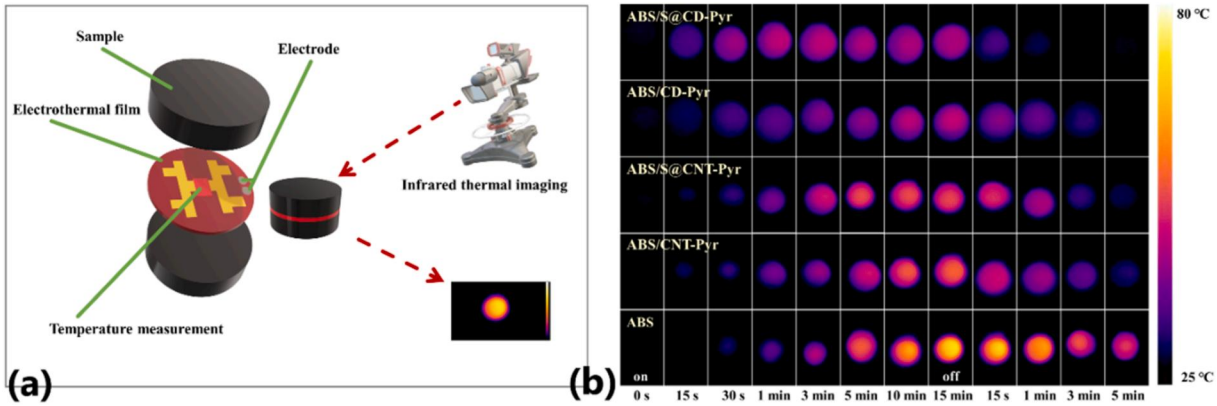

Fig. 7. The schematic diagram of the simulative heat diffusion experiment **(a)** and the changes of infrared thermal images for various polymer composites **(b)**.

some practical applications [67]. Thus, we recorded the electrical resistivity of polymer composites with respect to CDs or CNT fractions and filler's fraction (Fig. 8a and b). It can be found that as the increase of Pyr, CDs, or CNT, the electrical resistivity of most polymer composites showed decrease with varying degree, besides ABS/S@CD-Pyr. It exhibited an increased electrical resistivity as CDs fraction increased slightly and a much more slowly decrease as Pyr increased than that of other polymer composites, as evidenced by the greater electrical resistivity of ABS/S@CD-Pyr than 10^{11} Ω m. This was mainly attributed to the inherent structure of CDs as a polymer with ultra-short carbon chains and the strong electron-withdrawing effect of the polysulfide structure after sulfurization [68]. By contrast, ABS/CNT-Pyr and ABS/S@CNT-Pyr showed remarkable decrease with the increase of CNT and Pyr fractions due to the conductive networks of Pyr connected by conductive CNT. Although the sulfurization restricted the electron conduction, such an interconnected conductive network still greatly reduced the electrical insulation of polymer composites with CNT. Such an issue is often suffered from by most thermally conductive fillers, including graphene and metals [7]. These results indicated that ABS/S@CD-Pyr possessed great thermal conductivity and had excellent insulation performance.

3.6.3. The thermal stability

The thermal stability of polymer composites is a key characteristic for practical application and the high sulfur content and active surface of Pyr make it easier to combust and desulfurize during heating. We performed the TGA and DSC analyses of polymer composites to ascertain the thermal degradation rate and heat absorption/release (Fig. 8c and d). It can be found in Fig. 8c that ABS/S@CD-Pyr showed the greatest thermal stability with lower thermal loss rate than 0.5 wt% at 300 °C. By contrast, the thermal loss rate of waste ABS was 3.5 wt% at 300 °C. The results of DSC suggested that during the initial heating phase, all polymer composites showed a noticeable endothermic peak due to the heat absorption during the glass transition of the polymer matrix. Particularly, ABS/S@CNT-Pyr showed a much lower rate of heat absorption compared to the other counterparts. The reasons were the formed C–S and C═S and the presence of S-CDs, since the sulfur-bearing groups require the polymer to absorb more heat during the glass transition. When the temperature reached 180 °C, the heat absorption rate of waste ABS, ABS/S@CNT-Pyr, and ABS/CNT-Pyr rapidly decreased, and this exothermic reaction resulted from the gradual breaking and decomposition of polymer molecular chains. In comparison, the exothermic reaction of ABS/S@CD-Pyr was obviously weaker when the temperature was above 180 °C. This manifested that the C–S and C═S bonds formed within ABS/S@CD-Pyr endowed it with significant thermal resistance. Consequently, it was concluded that the presence of S-CDs clearly mitigated the inherent reactivity of Pyr, leading to good thermal stability of polymer composites.

3.6.4. The mechanical strength

For practical application, the mechanical strength of polymer composites is crucial for framing and structural materials. To evaluate the mechanical strength, the tensile tests of polymer composites were performed (Fig. 8e and f). The results indicated that all polymer composites showed similarly brittle fracture behaviors, while the maximum tensile strength was distinct. Specifically, the maximum strain before fracture for ABS/S@CD-Pyr was about 5.4 %, which was slightly lower than that of ABS/S@CNT-Pyr. This was mainly attributed to the superior elongation performance of CNT. Nevertheless, the chemical interactions (as proved above) induced by S-CDs compensated the shortcoming of ABS/

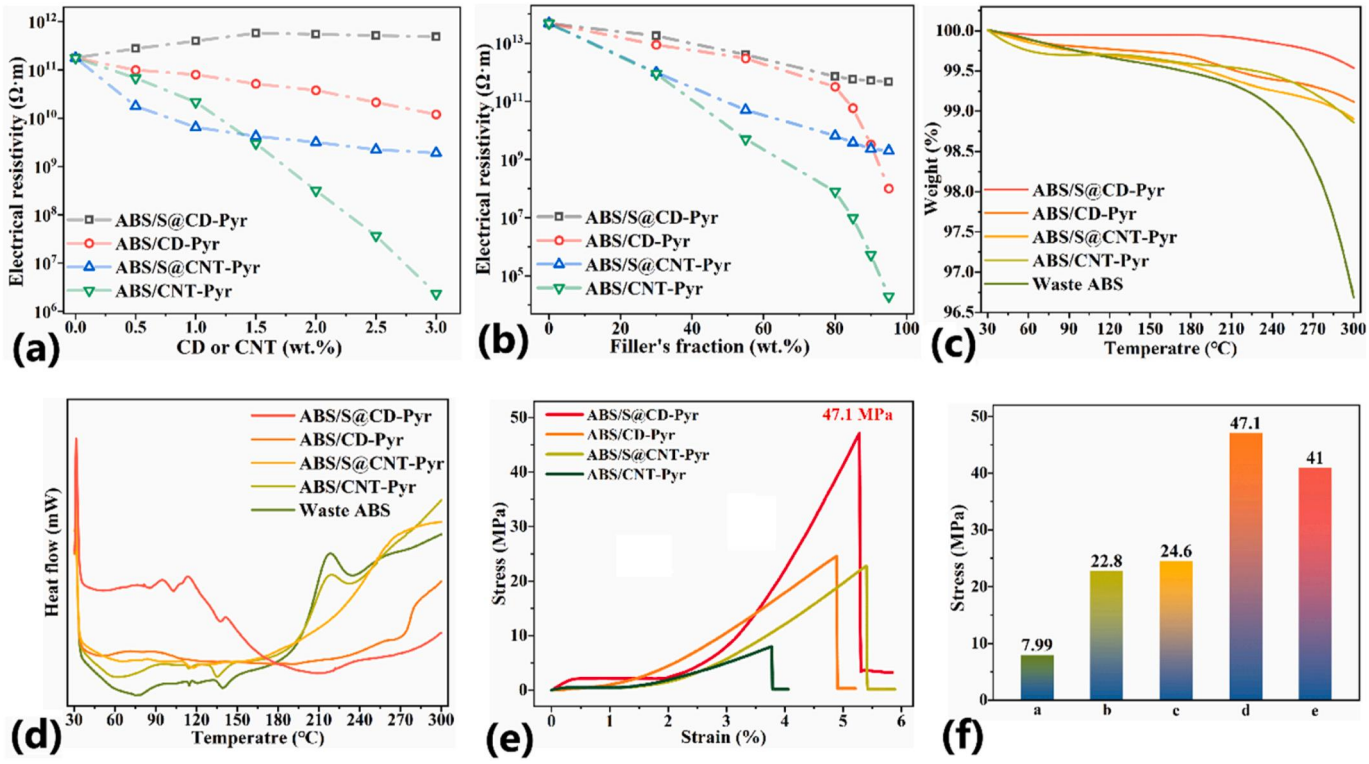

Fig. 8. The effect of CDs or CNT fraction **(a)** and filler's fraction **(b)** on the electrical resistivity of polymer composites; the TGA **(c)**, DSC **(e)**, typical stress-strain curve **(e)**, and the comparison of maximum stress **(f)** of polymer composites; in Fig. 8**f, a**, **b**, **c**, **d**, and **e** represent ABS/CNT-Pyr, ABS/S@CNT-Pyr, ABS/CD-Pyr, ABS/S@CD-Pyr, and commercial ABS, respectively.

S@CD-Pyr, endowing it with a comparable maximum strain. In order to analyze the differences of mechanical strength between ABS/S@CD-Pyr and the commercial frame materials of electrical and electronic equipment, we conducted the comparison of the maximum tensile strength of polymer composites and commercial ABS (Fig. 8f). The results showed that ABS/S@CD-Pyr possessed the greatest maximum tensile strength (41.7 MPa), particularly greater than that of commercial ABS. Such an increase in the maximum tensile strength of ABS/S@CD-Pyr highlighted the combined effect of S-CDs.

3.6.5. The surface hydrophobicity

Inherently, the water resistance of polymer materials is a natural advantage, while that of polymer composites can be affected by the fillers. Given that Pyr exhibited poor hydrophobicity due to the high-energy surface, it was envisioned to decrease the water resistance of polymer composites. Thus, the hydrophobicity of polymer composites along with Pyr were evaluated by measuring contact angle. It was observed in Fig. S9 that the contact angle of waste ABS and Pyr was 110.5° and 62.0°, in good agreement with their inherently hydrophobicity and hydrophilicity, respectively. After fabrication of polymer composites, the hydrophobicity was reduced slightly with the contact angle of 90.5°–107.0°. Particularly, the sulfuration reduced the contact angle of both ABS/S@CD-Pyr and ABS/S@CNT-Pyr due to the introduction of polar groups [69]. In contrast to waste ABS, the slightly decreased contact angle of polymer composites for ABS/S@CD-Pyr was attributed to the complete encapsulation of fillers and S-CDs by the polymer matrix, as confirmed by SEM. In conclusion, the surface of polymer composites still exhibited a higher contact angle than 90°, and thereby their water resistance was effective for practical application.

3.6.6. The EMI shielding performance

For application in automotive electronics, communications, and wearable devices, the EMI shielding is another crucial property of polymer composites [2]. In nature, the EMI shielding materials can address the electromagnetic interference caused by the increasing integration and high-speed signal transmission, and its effectiveness is generally affected by the magnetic and electrical shielding effect. In this case, the fillers with magnetic shielding are considered as the promising alternative, and as envisioned, Pyr is a magnetic mineral magnetically separated from pyrite ores [36]. Herein, the total absorption coefficient (SE_T), absorption coefficient (SE_A), and reflection coefficient (SE_R) of polymer materials were tested and calculated (**Section S3**). It was found that the EMI SE of ABS/S@CD-Pyr reached 43.1 dB, with a resistivity greater than 10^{11} Ω m (Fig. 9a). In addition, the SE_R of ABS/S@CD-Pyr accounted for only 2.64 % of SE_T, indicating that its EMI shielding effectiveness was largely dependent on absorption. Such a property endowed ABS/S@CD-Pyr with excellent EMI shielding effectiveness and high insulation performance. By contrast, the polymer composites with CNT showed a higher SE_R, but a relatively lower SE_T, suggesting that the EMI shielding of ABS/S@CNT-Pyr and ABS/CNT-Pyr mainly depended on reflection. Thus, the polymer composites with S-CDs showed great EMI shielding effectiveness. It is generally believed that materials with EMI reaching over 40 dB have moderate electromagnetic protection. ABS/S@CD-Pyr with EMI reaching 43.1 dB in the X-band (8–12 GHz) is expected to be applied in fields such as aviation lightweight components, precision instruments, satellite reflector substrates, and shielding coatings [70–73].

3.6.7. The performance of thermal cycling

In practical application, the thermally conductive polymers in electronics and electrical equipment generally suffered from frequent fluctuations in temperature between high and low extremes. The thermal degradation and other changes of polymer composites induced by the repeated thermal cycling can clearly affect the lifespan. Thus, the high-low temperature cycling for ABS/S@CD-Pyr between 25 °C and 100 °C was performed using an infrared thermometer to record the surface temperature. Note that one cycle included heating from 25 °C to 100 °C and then cooling back down to 25 °C. The results shown in Fig. 9b displayed the changes the TC of ABS/S@CD-Pyr with respect to the cycle number. At high temperatures (100 °C), the TC of ABS/S@CD-Pyr gradually increased and eventually stabilized as the cycle number increased; by contrast, the TC gradually decreased at low temperatures (25 °C). The reasons were that a small amount of incompletely formed polysulfide bonds would be completed by heat treatment at high temperature, resulting in a slightly increased TC; in contrast, at low temperature, the slightly decreased TC was mainly due to the irreversible molding shrinkage with the cycle number. However, the mobility of polymer chains at high temperature would mitigate the impact of such a shrinkage.

3.7. Environmental implications

Compared with other traditional fillers, using Pyr as a filler has significant environmental benefits [74]. Different filling systems can lead to significant differences in carbon emissions, and carbon emissions are the most direct indicator for evaluating the

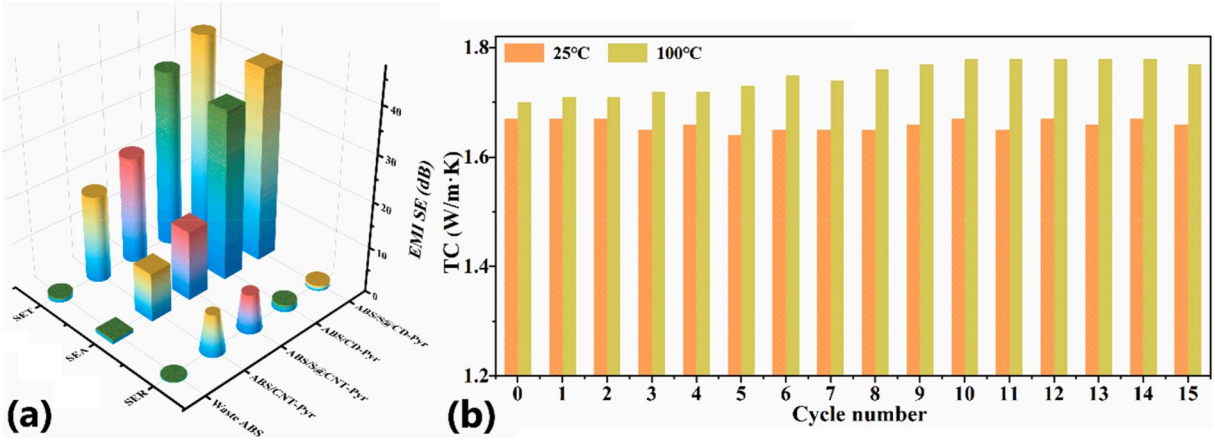

Fig. 9. The electromagnetic shielding effect coefficients of various polymer composites and raw materials **(a)** and thermal cycling experiment of ABS/S@CD-Pyr **(b)**.

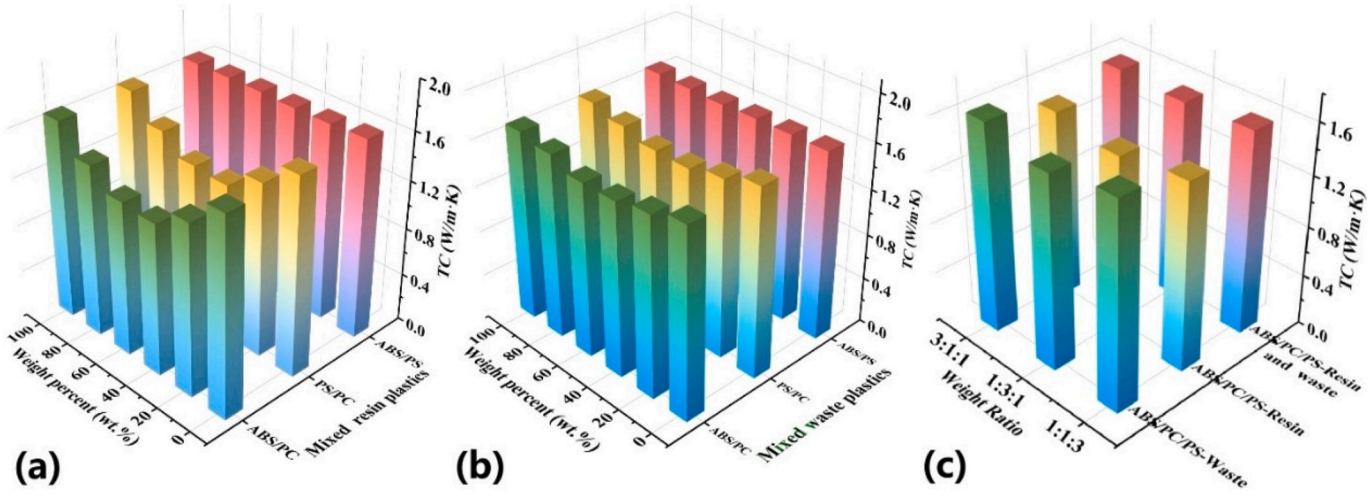

Fig. 10. The effect of plastic sources and types on the TC of polymer composites: **(a)** the mixed resin plastics, **(b)** the mixed waste plastics, and **(c)** the triple mixtures.

environmental benefits of a process. Therefore, we conducted a preliminary assessment of the direct carbon emissions (DCE) and indirect carbon emissions (ICE) of some fillers cited in this paper (Fig. S10). It can be seen that the ICE of different fillers is similar, and the main difference focus on the DCE. Some fillers have extremely high DCE due to harsh production conditions, while relatively mature filler systems have lower DCE. Due to the characteristics of the solid waste awaiting disposal in Pyr, the closed-loop utilization process has almost no DCE and only a small amount of ICE.

Due to durability and relatively low cost, plastics as one of the most widely used materials on the planet have resulted in the generation of immense waste plastics [75]. Most waste plastics are discarded, landfilled, and incinerated owing to the lack of effective recycling methods, severely aggravating environmental and resource crises [76]. Pyr as the associated mineral of sulfide mineral is considered a vital mineral waste in many mining situations, and has resulted in land occupation, severe soil acidification and erosion [77]. Currently, recycling of these bulk solid wastes, particularly for high-value products, is of significance with economic, social, and environmental benefits. Towards electronic packaging in 5G, we reported an efficient strategy to fabricate thermally conductive polymers using waste plastics and Pyr tailings, and elucidated the mechanisms of interface-coupling enhancement of CDs. First, the fabricated polymer composites exhibited prominent performance in thermal conductivity with TC of 1.68 W/m·K, greater than that of previously reported polymer composites using boron nitride, SiC nanowires, and fluorinated graphene aerogel as fillers in virgin resin [57,67,78]. Besides, the fabricated polymer composites possessed good electrical resistivity, EMI shielding performance, thermal stability, mechanical strength, thermal cycling, and water resistance. Second, the mechanisms of interface-coupling enhancement of CDs along with the interfacial interactions of components in polymer composites were elucidated using experiments and MD simulation. The strengthened interfacial chemical coupling and the nanometer size effect of CDs were mainly responsible for the enhanced thermal conductivity of polymer composites. Finally, to evaluate the applicability of strategy proposed in our study, we used various waste and pristine plastics (ABS, PS, and PC) to fabricate thermally conductive polymers under different weight ratio and combination (Fig. 10 and Fig. S11). It was found that in all cases, the TC of polymer composites was within the range of 1.23–1.67 W/m·K, indicating that the strategy proposed in our study exhibited broad applicability. The findings not only provided valuable theoretical framework for the design and application of thermally conductive polymers for electronic packaging, but also proposed novel strategies for recycling of waste plastics and Pyr tailings with environmental, economic and social benefits.

4. Conclusion

In this study, the polymer composites with high thermal conductivity were successfully fabricated via a dual interface strategy using both waste plastics and Pyr tailings, and the mechanisms of interface coupling enhanced by CDs were elucidated. The main conclusions can be made as follows:

- The TC of ABS/S@CD-Pyr was clearly affected by filler's fraction, K_2S_n concentration, CDs' fraction, and parameters in hot-pressing (time, temperature, and pressure); the highest TC of ABS/S@CD-Pyr reached 1.68 W/m·K;
- By introducing CDs, a homogeneous polymer matrix with uniformly distributed Pyr was fabricated; the enhanced interface coupling and nanoscale effects by CDs reduced the ITR and CTR and promoted thermal conductivity;
- ABS/S@CD-Pyr showed prominent performance in electromagnetic interference shielding and electrical resistivity; the EMI SE and electrical resistivity of ABS/S@CD-Pyr were 43.1 dB and greater than 10^{11} Ω m, respectively;
- ABS/S@CD-Pyr exhibited good thermal stability, mechanical strength, water resistance, and thermal cycling; particularly, the TC of ABS/S@CD-Pyr maintained stable after 15 times high-low temperature recycling;
- Using different types of waste and pristine plastics (ABS, PS, and PC), the most polymer composites fabricated under various weight ratio of dual and triple mixtures exhibited a greater TC than 1.6 W/m·K;

Overall, this study only provided valuable insights into the fabrication and application of polymer composites with high thermal conductivity towards modern electronic packaging, but also exhibited promising prospect for high-value and sustainable utilization of waste plastics and Pyr tailings.

CRediT authorship contribution statement

Zhiyi Wang: Writing – review & editing, Writing – original draft, Software, Resources, Data curation, Conceptualization.

Jianchao Wang: Writing – review & editing, Validation, Supervision. **Hui Wang:** Funding acquisition, Conceptualization. **Hongru Jiang:** Writing – review & editing, Supervision, Investigation. **Chongqing Wang:** Investigation, Formal analysis. **Yingshuang Zhang:** Writing – review & editing, Project administration. **Hongshuai Hou:** Conceptualization. **Lingyue Zhang:** Writing – review & editing.

Data availability

On request: Data is available to authors who reasonably request it.

Declaration of competing interest

The authors declare that they have no known competing financial interests or personal relationships that could have appeared to influence the work reported in this paper.

Acknowledgements

Funding: This work was supported by the National Natural Science Foundation of China (52300071) and Young Elite Scientist Sponsorship Program by BAST (BYESS2023097).

Appendix A. Supplementary data

Supplementary data to this article can be found online at https://doi.org/10.1016/j.aiepr.2025.09.006.

References

[1] Y. Wen, C. Chen, Y. Ye, Z. Xue, H. Liu, X. Zhou, Y. Zhang, D. Li, X. Xie, Y.-W. Mai, Advances on thermally conductive epoxy-based composites as electronic packaging underfill materials—A review, Adv. Mater. 34 (2022) 2201023.
[2] C. Zhao, Y. Li, Y. Liu, H. Xie, W. Yu, A critical review of the preparation strategies of thermally conductive and electrically insulating polymeric materials and their applications in heat dissipation of electronic devices, Adv. Compos. Hybrid Mater. 6 (2022) 27.
[3] X. Zhang, X. Zhang, M. Yang, S. Yang, H. Wu, S. Guo, Y. Wang, Ordered multilayer film of (graphene oxide/polymer and boron nitride/polymer) nanocomposites: an ideal EMI shielding material with excellent electrical insulation and high thermal conductivity, Compos. Sci. Technol. 136 (2016) 104–110.
[4] L. Zhang, H. Deng, Q. Fu, Recent progress on thermal conductive and electrical insulating polymer composites, Compos. Commun. 8 (2018) 74–82.
[5] X. Xu, J. Zhou, J. Chen, Thermal transport in conductive polymer–based materials, Adv. Funct. Mater. 30 (2020) 1904704.
[6] H. Chen, V.V. Ginzburg, J. Yang, Y. Yang, W. Liu, Y. Huang, L. Du, B. Chen, Thermal conductivity of polymer-based composites: fundamentals and applications, Prog. Polym. Sci. 59 (2016) 41–85.
[7] X. Sun, C. Huang, L. Wang, L. Liang, Y. Cheng, W. Fei, Y. Li, Recent progress in graphene/polymer nanocomposites, Adv. Mater. 33 (2021) 2001105.
[8] L. Wang, Q. Yao, H. Bi, F. Huang, Q. Wang, L. Chen, PANI/graphene nanocomposite films with high thermoelectric properties by enhanced molecular ordering, J. Mater. Chem. A 3 (2015) 7086–7092.
[9] L. Wang, Q. Yao, J. Xiao, K. Zeng, S. Qu, W. Shi, Q. Wang, L. Chen, Engineered molecular chain ordering in single-walled carbon nanotubes/polyaniline composite films for high-performance organic thermoelectric materials, Chem. Asian J. 11 (2016) 1804–1810.
[10] C. Pan, K. Kou, Y. Zhang, Z. Li, G. Wu, Enhanced through-plane thermal conductivity of PTFE composites with hybrid fillers of hexagonal boron nitride platelets and aluminum nitride particles, Compos. Part Eng. 153 (2018) 1–8.
[11] M.D. Joshi, A. Goyal, S.M. Patil, R.K. Goyal, Tribological and thermal properties of hexagonal boron nitride filled high-performance polymer nanocomposites, J. Appl. Polym. Sci. 134 (2016).
[12] G. Yıldız, M. Akkoyun, Thermal and electrical properties of aluminum nitride/boron nitride filled polyamide 6 hybrid polymer composites, J. Appl. Polym. Sci. 138 (2021).
[13] W. Lee, J. Kim, Highly thermal conductive and electrical insulating epoxy composites with a three-dimensional filler network by sintering silver nanowires on aluminum nitride surface, Polymers 13 (2021).
[14] X. Xu, J. Chen, J. Zhou, B. Li, Thermal conductivity of polymers and their nanocomposites, Adv. Mater. 30 (2018) e1705544.
[15] A. Gebrekrstos, S.S. Ray, Superior electrical conductivity and mechanical properties of phase-separated polymer blend composites by tuning the localization of nanoparticles for electromagnetic interference shielding applications, J. Polym. Sci. 61 (2023) 2567–2584.
[16] J.-N. Shi, M.-D. Ger, Y.-M. Liu, Y.-C. Fan, N.-T. Wen, C.-K. Lin, N.-W. Pu, Improving the thermal conductivity and shape-stabilization of phase change materials using nanographite additives, Carbon 51 (2013) 365–372.
[17] L. Chen, W. Li, Y. Liu, J. Leng, Nanocomposites of epoxy-based shape memory polymer and thermally reduced graphite oxide: mechanical, thermal and shape memory characterizations, Compos. Part Eng. 91 (2016) 75–82.
[18] J. Zhang, C. Li, C. Yu, X. Wang, Q. Li, H. Lu, Q. Zhang, J. Zhao, E. Songfeng, M. Hu, Y. Yao, Large improvement of thermal transport and mechanical performance of polyvinyl alcohol composites based on interface enhanced by SiO2 nanoparticle-modified-hexagonal boron nitride, Compos. Sci. Technol. 169 (2019) 167–175.
[19] Z. Wang, J. Su, J. Wang, Y. Feng, Q. Xu, H. Wang, H. Jiang, Unification of thermal conductivity, electrical insulation, and electromagnetic shielding: a bulk thermal conductive polymer from solid waste, Chem. Eng. J. 498 (2024) 155065.
[20] Y. Wang, Y. Liu, X. Hao, X. Zhou, H. Peng, Z. Shen, I.I. Smalyukh, X. Xie, B. Yang, Supramolecular liquid crystal carbon dots for solvent-free direct ink writing, Adv. Mater. 35 (2023) e2303680.
[21] Y. Shi, W. Su, F. Yuan, T. Yuan, X. Song, Y. Han, S. Wei, Y. Zhang, Y. Li, X. Li, L. Fan, Carbon dots for electroluminescent light-emitting diodes: recent progress and future prospects, Adv. Mater. 35 (2023) e2210699.
[22] Y. Lv, W. Zhao, Y. Qiang, J. Zhao, Constructing the interface of g-C3N4/epoxy composites using carbon quantum dots to achieve self-repairing, early corrosion monitoring and superior anticorrosion performance, Corros. Sci. 225 (2023) 111601.
[23] J.R. Seibert, Ö. Keleş, J. Wang, F. Erogbogbo, Infusion of graphene quantum dots to modulate thermal conductivity and dynamic mechanical properties of polymers, Polymer 185 (2019).
[24] S.Y. Son, H.N. Jo, M. Park, G.Y. Jung, D.S. Lee, S. Lee, H.I. Joh, Unusual thermal conductivity of carbon nanosheets with self-emerged graphitic carbon dots, ACS Appl. Mater. Interfaces 11 (2019) 13616–13623.
[25] Y. Zhou, S.K. Sharma, Z. Peng, R.M. Leblanc, Polymers in carbon dots: a review, Polymers 9 (2017).
[26] A. Alaghmandfard, O. Sedighi, N. Tabatabaei Rezaei, A.A. Abedini, A. Malek Khachatourian, M.S. Toprak, A. Seifalian, Recent advances in the modification of carbon-based quantum dots for biomedical applications, Mater. Sci. Eng. C Mater. Biol. Appl. 120 (2021) 111756.
[27] A. Chandrashekar, M. Hegde, S. Krishna, J. Ayippadath Gopi, T.M. Kotresh, T.N. Prabhu, Non-covalent surface functionalization of nanofillers towards the enhancement of thermal conductivity of polymer nanocomposites: a mini review, Eur. Polym. J. 198 (2023) 112379.
[28] H. Jiang, Q. Cai, S. Mateti, A. Bhattacharjee, Y. Yu, X. Zeng, R. Sun, S. Huang, Y.I. Chen, Recent research advances in hexagonal boron nitride/polymer nanocomposites with isotropic thermal conductivity, Adv. Nanocompos. 1 (2024) 144–156.
[29] J. Wang, C. Wang, Z. Cheng, C. Wang, D. Yue, H. Wang, H. Jiang, B. Jiang, L. Zhang, Exploring flotation separation of polycarbonate from multi-microplastic mixtures via experiment and numerical simulation, Chem. Eng. J. 474 (2023) 145854.
[30] J. Dehio, R. Janßen-Timmen, M. Rothgang, Regulating markets for post-consumer recycling plastics: experiences from Germany's dual system, Resour. Conserv. Recycl. 196 (2023) 107048.
[31] F. Zhan, H. Zhang, R. Cao, Y. Fan, P. Xu, J. Chen, Release and transformation of BTBPE during the thermal treatment of flame retardant ABS plastics, Environ. Sci. Technol. 53 (2018) 185–193.
[32] B. Sun, Y. Hu, H. Cheng, S. Tao, Kinetics of brominated flame retardant (BFR) releases from granules of waste plastics, Environ. Sci. Technol. 50 (2016) 13419–13427.
[33] X. Liu, X. Lu, Y. Feng, L. Zhang, Z. Yuan, Recycled WEEE plastics in China: generation trend and environmental impacts, Resour. Conserv. Recycl. 177 (2022) 105978.
[34] V. Nava, S. Chandra, J. Aherne, M.B. Alfonso, A.M. Antão-Geraldes, K. Attermeyer, R. Bao, M. Bartrons, S.A. Berger, M. Biernaczyk, R. Bissen, J.D. Brookes, D. Brown, M. Cañedo-Argüelles, M. Canle, C. Capelli, R. Carballeira, J.L. Cereijo, S. Chawchai, S.T. Christensen, K.S. Christoffersen, E. de Eyto, J. Delgado, T.N. Dornan, J.P. Doubek, J. Dusaucy, O. Erina, Z. Ersoy, H. Feuchtmayr, M.L. Frezzotti, S. Galafassi, D. Gateuille, V. Gonçalves, H.-P. Grossart, D.P. Hamilton, T.D. Harris, K. Kangur, G.B. Kankılıç, R. Kessler, C. Kiel, E.M. Krynak, À. Leiva-Presa, F. Lepori, M.G. Matias, S.-i.S. Matsuzaki, Y. McElarney, B. Messyasz, M. Mitchell, M.C. Mlambo, S.N. Motitsoe, S. Nandini, V. Orlandi, C. Owens, D. Özkundakci, S. Pinnow, A. Pociecha, P.M. Raposeiro, E.-I. Rõõm, F. Rotta, N. Salmaso, S.S.S. Sarma, D. Sartirana, F. Scordo, C. Sibomana, D. Siewert, K. Stepanowska, Ü.N. Tavşanoğlu, M. Tereshina, J. Thompson, M. Tolotti, A. Valois, P. Verburg, B. Welsh, B. Wesolek, G.A. Weyhenmeyer, N. Wu, E. Zawisza, L. Zink, B. Leoni, Plastic debris in Lakes and reservoirs, Nature 619 (2023) 317–322.
[35] L.E. Revell, P. Kuma, E.C. Le Ru, W.R.C. Somerville, S. Gaw, Direct radiative effects of airborne microplastics, Nature 598 (2021) 462–467.
[36] X.Q. Tang, Y. Chen, A review of flotation and selective separation of pyrrhotite: a perspective from crystal structures, Int. J. Min. Sci. Technol. 32 (2022) 847–863.

[37] C.L. Rodríguez-Corvera, A.L. Elías, A. Morelos-Gómez, M. Endo, E. Muñoz-Sandoval, F. López-Urías, Hybrid materials based on pyrrhotite, troilite, and few-layered graphitic nanostructures: synthesis, characterization, and cyclic voltammetry studies, Appl. Surf. Sci. 563 (2021) 150327.
[38] Q. Meng, Z. Yuan, Y. Du, J. Wang, Sulfuric acid pretreatment of oxidized pyrrhotite in flotation desulphurization of magnetite concentrate, Miner. Eng. 203 (2023).
[39] J. Liu, E.-l. Li, K. Jiang, Y.-j. Li, Y.-x. Han, Effect of acidic activators on the flotation of oxidized pyrrhotite, Miner. Eng. 120 (2018) 75–79.
[40] L. Yang, J. Zhao, C. Wang, R. Pang, D. Wang, X. Zhao, C. Chen, Significant enhancement of bi-directional ultrahigh thermal conductivity in polymer composites fabricated via polyetherimide@Silver core–shell structured microspheres, Chem. Eng. J. 500 (2024).
[41] H. Hou, L. Shao, Y. Zhang, G. Zou, J. Chen, X. Ji, Large-area carbon nanosheets doped with phosphorus: a high-performance anode material for sodium-ion batteries, Adv. Sci. 4 (2017) 1600243.
[42] C.-h. Zhao, B.-z. Wu, J.-h. Chen, Electronic structure and flotation behavior of monoclinic and hexagonal pyrrhotite, J. Cent. South Univ. 22 (2015) 466–471.
[43] L. Qiu, H. Zou, X. Wang, Y. Feng, X. Zhang, J. Zhao, X. Zhang, Q. Li, Enhancing the interfacial interaction of carbon nanotubes fibers by Au nanoparticles with improved performance of the electrical and thermal conductivity, Carbon 141 (2019) 497–505.
[44] T. Luo, J.R. Lloyd, Enhancement of thermal energy transport across graphene/graphite and polymer interfaces: a molecular dynamics study, Adv. Funct. Mater. 22 (2012) 2495–2502.
[45] J. Kruzelák, A. Kvasnicáková, K. Hlozeková, I. Hudec, Progress in polymers and polymer composites used as efficient materials for EMI shielding, Nanoscale Adv. 3 (2021) 123–172.
[46] S. Jasmee, G. Omar, S.S.C. Othaman, N.A. Masripan, H.A. Hamid, Interface thermal resistance and thermal conductivity of polymer composites at different types, shapes, and sizes of fillers: a review, Polym. Compos. 42 (2021) 2629–2652.
[47] B. Wang, Y.K. Chen, T.Q. Qu, F.M. Li, Structure and properties of multi-walled carbon nanotube/acrylonitrile butadiene styrene nanocomposite specimens prepared by fused deposition modeling, J. Macromol. Sci. B 60 (2021) 77–87.
[48] Y. Yu, P. Tang, B. Barnych, C. Zhao, G. Sun, M. Ge, Design and synthesis of core-shell carbon polymer dots with highly stable fluorescence in polymeric materials, ACS Appl. Nano Mater. 2 (2019) 6503–6512.
[49] A.M. Mirsaeidi, F. Yousefi, Viscosity, thermal conductivity and density of carbon quantum dots nanofluids: an experimental investigation and development of new correlation function and ANN modeling, J. Therm. Anal. Calorim. 143 (2021) 351–361.
[50] S.-Y. Yang, C.-C.M. Ma, C.-C. Teng, Y.-W. Huang, S.-H. Liao, Y.-L. Huang, H.-W. Tien, T.-M. Lee, K.-C. Chiou, Effect of functionalized carbon nanotubes on the thermal conductivity of epoxy composites, Carbon 48 (2010) 592–603.
[51] W. Yu, C. Liu, S. Fan, Advances of CNT-Based systems in thermal management, Nano Res. 14 (2021) 2471–2490.
[52] X.J. Wang, L.Z. Zhang, A randomly distributed filler model for heat conductivity prediction in filled composite materials considering fillers aggregation, Heat. Transfer. Eng. 36 (2015) 929–936.
[53] D.Y. Ren, C.D. Zhao, S.N. Zhang, K. Zhang, F.Q. Huang, A novel sulfur-containing carbon nanotubes with graphene nanoflaps for stretchable sensing, Joule heating, and electro-thermal actuating, Adv. Funct. Mater. 33 (2023) 2300517.
[54] Z. Deliballi, R. Demir-Cakan, B. Kiskan, Y. Yagci, Self-healable and recyclable sulfur rich Poly(vinyl chloride) by S-S dynamic bonding, Macromol. Chem. Phys. 224 (2023) 2100423.
[55] Z. Wang, F. Zhang, Y. Zhang, J. Su, H. Wang, H. Jiang, Turning waste and hazard into thermal conduction material: a promising destination of waste pyrrhotite and polystyrene, Constr. Build. Mater. 440 (2024).
[56] B.J. Wei, L. Zhang, S.Q. Yang, Polymer composites with expanded graphite network with superior thermal conductivity and electromagnetic interference shielding performance, Chem. Eng. J. 404 (2021) 126437.
[57] Y. Zhang, Y.F. Li, Q.X. Lei, X. Fang, H.Q. Xie, W. Yu, Tightly-packed fluorinated graphene aerogel/polydimethylsiloxane composite with excellent thermal management properties, Compos. Sci. Technol. 220 (2022) 109302.
[58] Z. Wang, Z. Wu, L. Weng, S. Ge, D. Jiang, M. Huang, D.M. Mulvihill, Q. Chen, Z. Guo, A. Jazzar, X. He, X. Zhang, B.B. Xu, A roadmap review of thermally conductive polymer composites: critical factors, progress, and prospects, Adv. Funct. Mater. 33 (2023).
[59] Y. Liao, D. Chen, S. Zou, S. Xiong, X. Xiao, H. Dang, T. Chen, S. Yang, Recyclable naturally derived magnetic pyrrhotite for elemental mercury recovery from flue gas, Environ. Sci. Technol. 50 (2016) 10562–10569.
[60] J. Wang, D. Yue, H. Wang, *In situ* Fe3O4 nanoparticles coating of polymers for separating hazardous PVC from microplastic mixtures, Chem. Eng. J. 407 (2021) 127170.
[61] Y.L. Botero, A. Canales-Mahuzier, R. Serna-Guerrero, A. López-Valdivieso, M. Benzaazoua, L.A. Cisternas, Physical-chemical study of IPETC and PAX collector's adsorption on covellite surface, Appl. Surf. Sci. 602 (2022).
[62] A.L. Muller, R.S. Picoloto, P. de Azevedo Mello, M.F. Ferrao, M. de Fatima Pereira dos Santos, R.C. Guimaraes, E.I. Muller, E.M. Flores, Total sulfur determination in residues of crude oil distillation using FT-IR/ATR and variable selection methods, Spectrochim. Acta 89 (2012) 82–87.
[63] P. Zhao, H. Cheng, H. Liu, J. Liu, K. Song, H. Hu, Unleashing the potential of sulfur-incorporated polymer framework composite for enhanced performance and stability of lithium-organosulfur batteries, J. Alloys Compd. 1003 (2024).
[64] S. Yang, Q. Sun, Sulfur-containing polymers for enhancing rate and cycle performance of lithium-sulfur batteries, J. Ind. Eng. Chem. 143 (2024) 144–150.
[65] H. Feng, Z. Liu, F. Wang, L. Xue, L. Li, C. Ye, C. Zhang, Q. Liu, J. Tan, The C—S/C═S bonds synergistically modify porous hollow-carbon-nanocages anode for durable and fast sodium-ion storage, Adv. Funct. Mater. 34 (2024).
[66] J. He, Y. Xia, W. Lin, K. Pal, Y. Zhu, M.G. Kanatzidis, C. Wolverton, Accelerated discovery and design of ultralow lattice thermal conductivity materials using chemical bonding principles, Adv. Funct. Mater. 32 (2021) 2108532.
[67] X.W. Wang, P.Y. Wu, Melamine foam-supported 3D interconnected boron nitride nanosheets network encapsulated in epoxy to achieve significant thermal conductivity enhancement at an ultralow filler loading, Chem. Eng. J. 348 (2018) 723–731.
[68] M. Han, C.E. Shuck, R. Rakhmanov, D. Parchment, B. Anasori, C.M. Koo, G. Friedman, Y. Gogotsi, Beyond Ti(3)C(2)T(x): Mxenes for electromagnetic interference shielding, ACS Nano 14 (2020) 5008–5016.
[69] J. Wang, H. Wang, D. Yue, Insights into mechanism of hypochlorite-induced functionalization of polymers toward separating BFR-containing components from microplastics, ACS Appl. Mater. Interfaces 12 (2020) 36755–36767.
[70] K. Sun, L. Wang, Z. Wang, X. Wu, G. Fan, Z. Wang, C. Cheng, R. Fan, M. Dong, Z. Guo, Flexible silver nanowire/carbon fiber felt metacomposites with weakly negative permittivity behavior, Phys. Chem. Chem. Phys. 22 (2020) 5114–5122.
[71] K. Sun, C. Wang, J. Tian, Z. Zhang, N. Zeng, R. Yin, W. Duan, Q. Hou, Y. Zhao, H. Wu, R. Fan, Magnetic-driven broadband epsilon-near-zero materials at radio frequency, Adv. Funct. Mater. 34 (2023).
[72] M. Liu, H. Wu, Y. Wu, P. Xie, R.A. Pashameah, H.M. Abo-Dief, S.M. El-Bahy, Y. Wei, G. Li, W. Li, G. Liang, C. Liu, K. Sun, R. Fan, The weakly negative permittivity with low-frequency-dispersion behavior in percolative carbon nanotubes/epoxy nanocomposites at radio-frequency range, Adv. Compos. Hybrid Mater. 5 (2022) 2021–2030.
[73] K. Sun, Z. Xie, X. Yang, Y. Long, P. Yang, C. Cheng, X. Qi, Enhanced microwave absorption in C@Co/carbonyl iron fiber composite with multi-level interfaces, Adv. Compos. Hybrid Mater. 8 (2024).
[74] Z. Wang, F. Zhang, Y. Zhang, J. Su, H. Wang, H. Jiang, Turning waste and hazard into thermal conduction material: a promising destination of waste pyrrhotite and polystyrene, Constr. Build. Mater. 440 (2024).
[75] M.P. Drewniok, Y. Gao, J.M. Cullen, A. Cabrera Serrenho, What to Do about plastics? Lessons from a study of United Kingdom plastics flows, Environ. Sci. Technol. 57 (2023) 4513–4521.
[76] P.A. Kots, B.C. Vance, C.M. Quinn, C. Wang, D.G. Vlachos, A two-stage strategy for upcycling chlorine-contaminated plastic waste, Nat. Sustain. 6 (2023) 1258–1267.
[77] J. He, B. Zhang, Y. Wang, S. Chen, H. Dong, Vanadate bio-detoxification driven by pyrrhotite with secondary mineral formation, Environ. Sci. Technol. 57 (2023) 1807–1818.
[78] W. Dai, J.H. Yu, Z.D. Liu, Y. Wang, Y.Z. Song, J.L. Lyu, H. Bai, K. Nishimura, N. Jiang, Enhanced thermal conductivity and retained electrical insulation for polyimide composites with SiC nanowires grown on graphene hybrid fillers, Compos. Part. A-Appl. S 76 (2015) 73–81.